MOLECULAR AND CELLULAR BIOLOGY, Nov. 1987, p. 4048–4057
0270-7306/87/114048-10$02.00/0

Vol. 7, No. 11

Amino Acid Sequences That Determine the Nuclear Localization of Yeast Histone 2B

ROBERT B. MORELAND,[1,2]† * GARY L. LANGEVIN,[3] ROBERT H. SINGER,[3] ROBERT L. GARCEA,[2] AND LYNNA M. HEREFORD[1]

Laboratory of Gene Regulation,[1] and the Division of Pediatric Oncology,[2] Dana Farber Cancer Institute, Boston, Massachusetts 02115, and the Department of Anatomy, University of Massachusetts Medical School, Worcester, Massachusetts 01605[3]

Received 2 February 1987/Accepted 14 August 1987

Histone-β-galactosidase protein fusions were used to identify the domain of yeast histone 2B, which targets this protein to the nucleus. Amino acids 28 to 33 in H2B were required for nuclear localization of such fusion proteins and thus constitute a nuclear localization sequence. The amino acid sequence in this region (Gly-29 Lys Lys Arg Ser Lys Ala) is similar to the nuclear location signal in simian virus 40 large T antigen (Pro-126 Lys Lys Lys Arg Lys Val) (D. Kalderon, B. L. Roberts, W. D. Richardson, and A. E. Smith, Cell 39:499–509, 1984). A point mutation changing lysine 31 to methionine abolished nuclear localization of an H2B-β-galactosidase fusion protein containing amino acids 1 to 33 of H2B. However, an H2B-β-galactosidase fusion protein containing both this point mutation and the H2A interaction domain of H2B was nuclear localized. These results suggest that H2A and H2B may be cotransported to the nucleus as a heterodimer.

The biological importance of histones has led to a detailed knowledge of the primary sequence and functional domains of these proteins. The four core histones, H2A, H2B, H3, and H4, have a similar overall structure consisting of basic amino and carboxy termini and a globular hydrophobic internal region (for reviews, see references 23 and 33). The amino terminus of H2B is followed by a region of hydrophobic amino acids which has been identified as the minimal domain which interacts with H2A to form H2A-H2B dimers (amino acids 40 to 117 in *Saccharomyces cerevisiae* H2B; 37, 51). H2B is the least conserved of the four core histones, with most of the variability occurring at the amino terminus. Amino acids 3 to 32 or 30 to 37 can be deleted from yeast H2B without impairment of cell growth (46, 52). These studies suggest either that there is no obligatory biological requirement for the H2B amino terminus or that the function(s) of this domain can be complemented by other histones in the nucleosome.

During the period of yeast histone biosynthesis in late G1 and early S phase (20, 22, 39), approximately 4.0×10^5 histones per haploid genome are synthesized, transported into the nucleus, and assembled into nucleosomes. The number of histones which must be imported during the interval of DNA replication, as well as the requirement for their precise stoichiometry in nucleosome assembly, suggests that specific transport mechanisms are used in histone nuclear localization.

The transport of proteins into the nucleus can result from either passive diffusion through nuclear pores (4, 6, 40, 42) and accumulation in the nucleus by mass action (9) or by transport processes requiring recognition of an imported protein coupled to its active transport or facilitated diffusion (5, 10–12, 15, 19, 25, 26, 28, 29, 47). The existence of nuclear transport processes has been implicated in the nuclear localization of the *Xenopus* oocyte protein nucleoplasmin (11, 12). A specific carboxy-terminal domain has been shown to be required for nuclear uptake of pentameric nucleoplasmin oligomers (11). Moreover, gold particles as large as 20 nm which have been coated with nucleoplasmin have been observed to traverse nuclear pores (12). Since these particles are too large to diffuse through the pores (4, 6, 40, 42), specific transport mechanisms might be used in their uptake. Amino acid sequences required for nuclear localization have been identified in regions of yeast α-2 mating type protein (19), yeast GAL4 protein (47), yeast ribosomal protein L3 (36), simian virus 40 (SV40) large T antigen (25, 26, 28), and polyomavirus large T antigen (44). The nuclear location signal in SV40 large T antigen has been delimited to the eight amino acids from proline 126 to valine 133, and a single amino acid change can prevent the SV40 large T antigen from localizing in the nucleus (25, 28). Fusion of this sequence to chicken pyruvate kinase (26), albumin, immunoglobulin (15, 29), and ferritin (29) enables the nuclear localization of these large, otherwise cytoplasmic proteins.

We have identified an amino acid sequence in yeast H2B which is required for nuclear localization. Because a single amino acid substitution in this sequence abolished nuclear localization, this sequence may constitute a specific nuclear localization signal. Interestingly, this sequence occurs in the region of H2B that can be deleted without impairment of cell growth (46, 52). The implications of this latter finding with regard to cotransport of an H2A-H2B dimer are discussed.

MATERIALS AND METHODS

Strains and media. *Escherichia coli* LG90 (*F⁻*, Δ*lacz proXIII*; 17) was used for transformation and propagation of recombinant plasmids. Strain JM103 (*lac pro thi rpsL endA sbcB15 hsd-15 supEF' traD36 proAB lacI^qZ M15*) was used in M13 cloning (35). Bacterial transformation was carried out as reported previously (38). Strains were grown in L broth (LG90) or in 2XYT (JM103). *S. cerevisiae* GRF167 (*his3 ura3 MATα*) and DN102 (*his3 ura3 leu2 MATα*) were used in this work. DN102 is isogenic with GRF167. Typically, yeast transformations were done by using 5 to 10 μg of plasmid DNA as reported previously (24). Transformants were

* Corresponding author.
† Present address: Pediatric Oncology Research, Dana Farber Cancer Institute, Boston, MA 02115.

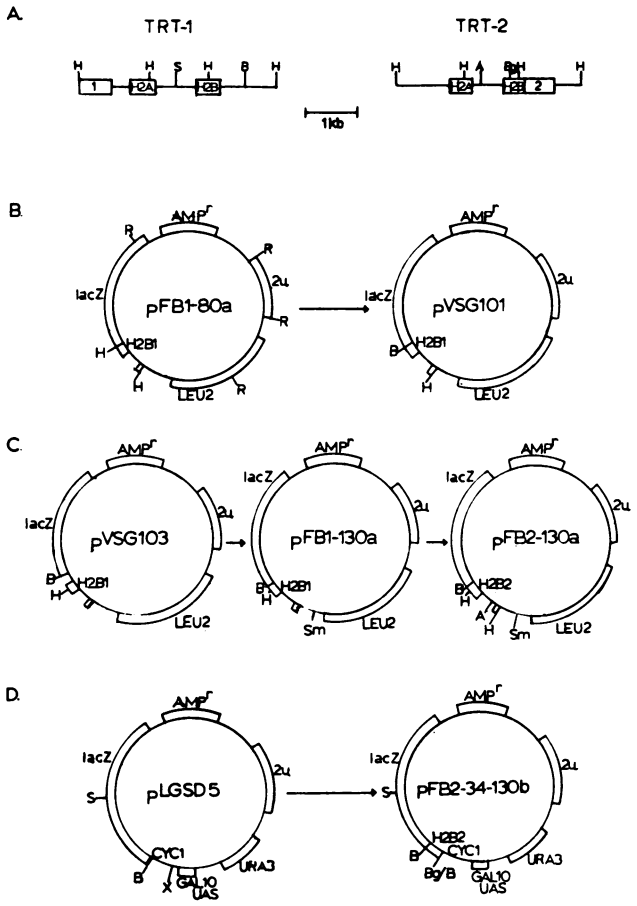

FIG. 1. Construction of H2B-β-galactosidase fusion plasmids. Panels: A, partial restriction map of the *TRT1* and *TRT2* loci (21); B, construction of pVSG101 (this vector was used to clone *H2B-lacZ* fusion genes containing 7 to 67 codons of *H2B*); C, construction of pVSG103, pFB1-130a, and pFB2-130a; D, construction of pFB2-34-130c. Restriction sites: *Acc*I (A), *Bam*HI (B), *Bgl*II (Bg), *Eco*RI (R), *Hin*dIII (H), *Sac*I (S), *Sma*I (Sm), and *Xho*I (X).

grown on minimal media lacking the essential component (leucine or uracil) used in selection.

Plasmid constructions. *S. cerevisiae* contains two divergent H2A-H2B gene pairs, *TRT1* and *TRT2* (21). H2B1 (*TRT1*) differs from H2B2 (*TRT2*) by four amino acid changes: alanine 2 to serine, lysine 3 to alanine, threonine 27 to valine, and alanine 35 to valine (51). *H2B-lacZ* fusion plasmids were named functionally according to the gene fusions they encode, e.g., pF (fusion) B (H2B) 1 (H2B1) or 2 (H2B2), followed by the number of histone codons in the *lacZ* fusion, followed by "a" when containing the yeast plasmid 2μm circle autonomous replicating sequence (2μm *ars*), "b" when containing the *CYC1* promoter regulated by the *GAL10* upstream activating sequence and methionine start codon (18), or "c" when containing the *GAL10* upstream activating sequence and a 2μm *ars*.

Methods used in recombinant plasmid construction have been previously reported (31). Since *H2B-lacZ* fusion genes are transcribed in *E. coli* (39), in-frame *H2B-lacZ* gene fusions were selected by expression of β-galactosidase using MacConkey plates (17). The plasmid pfusB1-5 was generated by subcloning the 1.1-kilobase (kb) *Hin*dIII fragment from the *TRT1* intergenic region (Fig. 1A) into a fusion vector (17, 39). A 2μm *ars* lacking a *Hin*dIII site was prepared by the insertion of an *Eco*RI synthetic linker into the *Hin*dIII site of the 2-kb *Hin*dIII-*Eco*RI 2μm fragment from Yep24 (7) and subsequently subcloned into the *Eco*RI site between the Amp^r and *LEU2* genes on plasmid pfusB1-5 to generate pFB1-80a (Fig. 1B). The fusion vector pVSG101 was then constructed by insertion of a *Bam*HI decamer linker into the filled-in *Hin*dIII site at the *H2B-lacZ* junction of pFB1-80a. The *Bam*HI site at the 5′ end of *lacZ* is in the same reading frame found in fusion genes on pLGSD5 (18) and pJT24 (13) (GGA TCC; Fig. 1B).

BAL 31 deletions (31) were prepared by using the 1.1-kb *Hin*dIII fragment from *TRT1*. Deletions were initiated from the *Hin*dIII site at codon 80 in the *H2B*-coding sequence, and following insertion of *Bam*HI octomer linkers, 1.0-kb and smaller *Hin*dIII-*Bam*HI fragments were isolated and subcloned into pVSG101. After transformation of bacteria and selection for in-frame β-galactosidase fusions, suitable deletion plasmids were selected by restriction analysis and size estimation on 10% acrylamide gels. Precise deletion endpoints were determined after subcloning deletion fragments into M13 vectors (35) and DNA sequencing by the dideoxy chain termination method (45). The lysine-31-to-methionine change was introduced into the 1.0-kb *H2B Hin*dIII-*Bam*HI fragment subcloned into M13 (33) by oligonucleotide-directed mutagenesis (14) using the 20-mer 5′ CTGATGGTAAGATGAGAAGC 3′. The presence of the mutated base pair was screened by DNA sequencing (45). The 1.0-kb *Hin*dIII-*Bam*HI fragment containing the mutation was then subcloned into pVSG101.

The fusion vector pVSG102 was constructed by filling in the *Hin*dIII site at codon 13 of the *H2A1* gene in pFB1-80a and then subcloning the 1.3-kb *Hin*dIII fragment from the *TRT1* locus (Fig. 1A) (21) into the remaining *Hin*dIII site. The *Hin*dIII site at the *lacZ* junction was filled in by using T4 DNA polymerase, and a *Bam*HI decamer linker was inserted to generate pVSG103 (Fig. 1C). The plasmid pFB1-130a was constructed by first introducing a *Bam*HI linker 3′ to codon 130 in *H2B1* by oligonucleotide-directed mutagenesis (14) using the 20-mer 5′ TCAAGCAGGATCCTAAGTCA 3′. The 150-base-pair (bp) *Hin*dIII-*Bam*HI piece encoding amino acids 80 to 130 was then subcloned into the 18.6-kb *Hin*dIII-*Bam*HI fragment of pVSG103. The plasmid pFB2-130a was constructed by subcloning a 2.6-kb *Sma*I-*Hin*dIII fragment from pFB2-80a into the 15.8-kb *Sma*I-*Hin*dIII fragment of pFB1-130a. This reconstructs the *Hin*dIII site on the *H2A1* side of the divergent promoter. The plasmid pFB2-80a is identical to pFB1-80a except that it contains the 0.97-kb *Hin*dIII fragment from the *TRT2* intragenic region (Fig. 1A). To construct pFB1-130K31→Ma, a lysine-31-to-methionine change was introduced into the 1.1-kb *Hin*dIII *TRT1* piece by oligonucleotide-directed mutagenesis as described above. After clones were sequenced (45), the full-length *H2B1* gene was reconstituted by virtue of the internal *Hin*dIII site at codon 80 by using the 18.5-kb *Hin*dIII fragment of pFB2-130a. Clones containing pFB1-130K31→Ma were verified by using restriction map differences in the *H2B1* and *H2B2* promoters (*Sac*I-*TRT1*, *Acc*I-*TRT2*; Fig. 1A).

Plasmid pFB2-33a was generated by subcloning a 0.95-kb *TRT2 Hin*dIII-*Bgl*I piece (Fig. 1A) into the 17.1-kb *Hin*dIII-*Bam*HI fragment of pVSG101. Fusions of the first 33 codons of *H2B2* containing a deletion of codons 2 through 22 were prepared by first inserting *Hin*dIII linkers into the *Eco*RI site at the second codon of the *H2A2* gene in plasmid p26-8 (51). A *Hin*dIII-*Bgl*II fragment containing the first 33 codons of *H2B2* and the deletion were subcloned into the 17.1-kb *Hin*dIII-*Bam*HI fragment from pVSG101. Both pFB2-130

Δ2-22a and pFB2-130 Δ14-32a were constructed by subcloning the 0.96-kb *Hin*dIII fragments from *Hin*dIII linker insertions at the second codon of the *H2A2* gene in plasmids p26-8 (2-22 deletion) and p28-8 (14-32 deletion; 50) into the 17.1-kb *Hin*dIII fragment from pFB2-130a.

Both pFB2-34-80b and pFB2-34-130b were constructed by subcloning the 2.2-kb *Bgl*II-*Sac*I fragment from pFB2-80a or the 2.4-kb *Bgl*II-*Sac*I fragment from pFB2-130a into the 11.0-kb *Bam*HI-*Sac*I fragment from pLGSD5 (Fig. 1D; 18). The 80-to-130-amino-acid *H2B1* fusion (pFB1-80-130b) was constructed by subcloning a filled-in *Hin*dIII-*Sac*I fragment from pFB1-130a into an 11.0-kb filled-in *Bam*HI-*Sac*I fragment from pLGSD5. All of these constructions are galactose regulated by virtue of the *GAL10* upstream activating sequence upstream of the *CYC1* promoter and contain the *CYC1* methionine start codon (18).

Galactose-regulated *H2B-lacZ* fusions were constructed by subcloning the appropriate filled-in *Sac*I-*Bam*HI fragments into *Sma*I-*Bam*HI-cut pJT24 (13). The *Sac*I site is 371 bp 5′ to the *H2B1* methionine start codon (38).

Plasmids containing the SP6 promoter were constructed by subcloning the 5.8-kb *Bam*HI-*Xmn*I fragment from pLG669-Z (18) containing all of *lacZ* into the 1.1-kb *Bam*HI-*Xmn*I fragment of pSP64 (34). The resulting plasmid, pSPZ, allows the cloning of β-galactosidase fusion genes that can be transcribed and translated in vitro by virtue of the SP6 promoter. The plasmid pSPRR was constructed by subcloning a 237-bp *Xba*I-*Bam*HI fragment from pTCM-RR (36) into *Xba*I-*Bam*HI-cut pSPZ. When RNA generated from *Tth*111-I-linearized pSPRR is translated in vitro, a fusion protein consisting of five amino acids of ribosomal protein L3 fused to β-galactosidase is produced. This protein was used as a β-galactosidase control in DNA-binding experiments (see below). The vector pSPZA was identical to pSPZ with the exception of the insertion of a poly(A) sequence that was subcloned into the T4 polymerase filled-in *Tth*111-I site 1.5 kb 3′ to the end of the *lacZ* gene (H. Fried, personal communication). This plasmid has a unique *Xho*I site 3′ to the poly(A) tract which can be used to linearize the plasmid to make full-length RNAs of fusion genes. Both pSPZA33 and pSPZA33K31→M were constructed by first ligating a *Hin*dIII linker to the *Taq*I site 64 bp 5′ to the H2B start codon in pFB1-33b and pFB1-33K→Mb, respectively. The resulting 163-bp *Hin*dIII-*Bam*HI fragments encoding the first 33 amino acids of H2B were subcloned into *Hin*dIII-*Bam*HI-cut pSPZA. The plasmid pSPZA130 containing the entire H2B-coding sequence was constructed by cloning a mung bean nuclease-digested *Taq*I-*Bam*HI 464-bp fragment from pFB1-130c into mung bean nuclease-digested *Hin*dIII-*Bam*HI-cut pSPZA. This plasmid was used for the production of H2B mRNA (linearized at the *Bam*HI site) or 130-amino-acid H2B-β-galactosidase fusion protein mRNA (linearized at the *Xho*I site).

Indirect immunofluorescence, immunoprecipitations, and Western blot analysis. The techniques used for indirect immunofluorescence (1) as well as immunoprecipitation of β-galactosidase fusion proteins have been previously described (36). Western blot (immunoblot) analysis was done on the fusion protein samples after sodium dodecyl sulfate (SDS)-polyacrylamide gel electrophoresis on 7.5% gels (50) by using affinity-purified rabbit anti-β-galactosidase antibodies and alkaline phosphatase-conjugated goat anti-rabbit immunoglobulin G antibodies (3, 30).

Immunocytochemical staining and electron microscopy. Affinity-purified rabbit anti-β-galactosidase immunoglobulin G was used as the primary antibody. The secondary antibody was a goat anti-rabbit immunoglobulin G antibody labeled with 10-nm colloidal gold particles (GARG10; Jannsen Life Science Products). This preparation was centrifuged at 700 × *g* for 10 min before use to remove aggregates. All solutions were filtered through 0.45-μm-pore-size filters before use.

Yeast cells containing the appropriate plasmids were grown on selective media containing 1.4% galactose plus 0.6% glucose (pFB1-33c and pFB1-33K-Mc) or 2% galactose (pLGSD5, pFB1-7c, and pFB1-67c). Cells were harvested in mid-log phase and were fixed in 1% glutaraldehyde in 60 mM potassium phosphate–1 mM magnesium chloride, pH 6.5, for 20 min. Cells were washed in phosphate-buffered saline and dehydrated through a series of increasing concentrations of ethanol. Pellets were then transferred to beem capsules, suspended, and pelleted through propylene oxide-Epon 812 resin (Tousimis Research Corp.).

An alternative protocol involved postfixing cells with 1% OsO_4 in phosphate-buffered saline for 30 min followed by dehydration via the ethanol series. Under these conditions, the cells would stick together after osmification and were processed as a hard pellet through infiltration. Pellets were embedded in flat molds (Ernest F. Fullam, Inc.).

Sectioning and staining procedures were performed at 22°C unless noted. Thin sections were cut on an LKB Instruments, Inc., Ultratome III or an Ivan Sorvall, Inc., MT-1 and were collected on gold grids (Fullam). Sections were etched for 20 min with 10% hydrogen peroxide (16), rinsed with water (20 drops per grid), and incubated in 8% bovine serum albumin in 50 mM Tris chloride–150 mM NaCl (pH 7.4). Sections were stained overnight at 4°C with a 1/100 dilution of the primary antibody in wash solution (1% bovine serum albumin, 0.1% Triton X-100, Tris-buffered saline, pH 7.4). The sections were washed in the same solution for 30 min on a stirring platform. Sections were incubated with gold-conjugated second antibody (1/100 in wash solution) for 2.5 h. The sections were then washed for 30 min in wash solution followed by a 10-min wash in Tris-buffered saline and finally a 30-min fixation in 1% glutaraldehyde-Tris-buffered saline. The grids were then individually washed in water and stained with 3% uranyl acetate followed by 0.2% lead citrate. When OsO_4 postfixed material was used, the hydrogen peroxide step was replaced with a 1-h incubation in a freshly made saturated aqueous solution of sodium metaperiodate (2). Sections were observed with a JEOL, Ltd. 100S microscope at 60 kV or at 80 kV for Formvar-stabilized sections.

DNA-binding experiments. mRNA was transcribed from *Tth*111-I-linearized pSPRR, *Xho*I-linearized pSPZA33, pSPZA33K→M, and pSPZA130, and *Bam*HI-linearized pSPZA130 by using SP6 RNA polymerase (34). The RNA was translated in a rabbit reticulocyte translation system including [^{35}S]methionine. An entire 50-μl translation reaction was used for each assay of DNA binding. Samples were equilibrated with 1-ml columns (600 μg of DNA) of double-stranded (ds) calf thymus DNA cellulose in 20 mM NaCl–20 mM EDTA–50 mM Tris chloride, pH 7.4 (loading buffer), on ice. The columns were washed with three volumes of the loading buffer and eluted stepwise with increasing concentrations of NaCl. Fusion proteins were then immunoprecipitated with β-galactosidase antibodies and electrophoresed on 7.5% SDS-polyacrylamide gels. Gels were dried and autoradiographed. Purified yeast H2B (32) or in vitro-translated H2B was bound to dsDNA cellulose and eluted as described above. Column fractions were precipitated with cold 20% trichloroacetic acid by using 5 μg of bovine serum albumin as carrier. Samples were electrophoresed on 15%

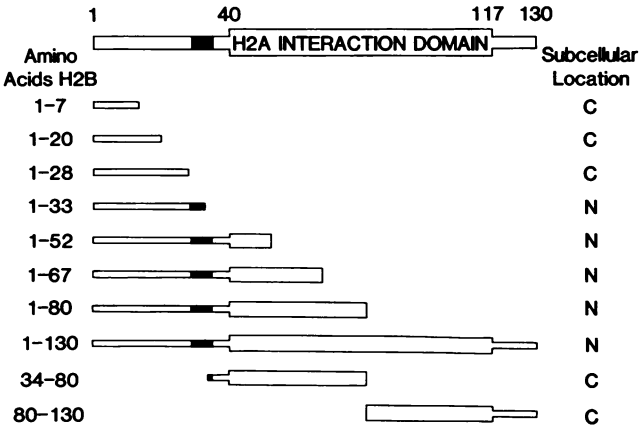

FIG. 2. Summary of the subcellular localization of H2B-β-galactosidase fusion proteins. The schematic diagram of H2B shows the nuclear localization sequence (black box) and the H2A interaction domain (33, 37, 51). Subcellular location determined by indirect immunofluorescence was either nuclear (N) or cytoplasmic (C). Constructions are described in Materials and Methods (Fig. 1).

SDS-polyacrylamide gels. The gels were either subjected to Western blot analysis (50) by using rabbit anti-yeast H2B antibody (gift of Tillman Schuster and Ulrich Certa) and alkaline phosphatase-conjugated goat anti-rabbit immunoglobulin G antibodies (3, 30) as with purified H2B, or else they were dried and autoradiographed (in vitro-translated H2B).

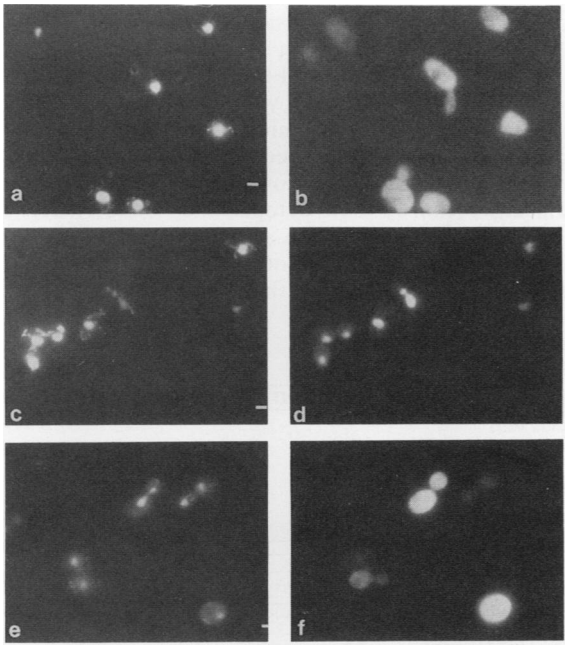

FIG. 3. Localization of H2B-β-galactosidase fusion proteins by indirect immunofluorescence. Panels: a and b, β-galactosidase alone; c and d, 33-amino-acid H2B-β-galactosidase fusion protein; e and f, 33-amino-acid H2B-β-galactosidase fusion with a lysine-31-to-methionine substitution. 4',6-Diamidino-2-phenylindole-stained fields (panels a, c, and e) show location of nuclei and mitochondria, and the corresponding fluorescein-stained fields (panels b, d, and f) show β-galactosidase subcellular localization. The results shown are typical of cytoplasmic- and nuclear-localized proteins. Bar, 5.0 μm.

RESULTS

Defining H2B nuclear localization sequences. To detect a nuclear localization sequence in yeast H2B, chimeric *H2B*-β-galactosidase (*lacZ*) gene fusions were constructed by fusing the yeast H2B promoter and coding sequences to the amino terminus of *lacZ*. The subcellular locations of the hybrid fusion proteins produced in yeast were then determined by indirect immunofluorescence using anti-β-galactosidase antibodies. In the initial analysis, progressive deletions from the carboxy terminus of H2B were constructed and fused to the β-galactosidase gene (Fig. 2). Indirect immunofluorescence of cells producing these fusion proteins showed either cytoplasmic or nuclear localization of β-galactosidase (Fig. 3). The transition from a nuclear-localized to a cytoplasmically localized fluorescence phenotype was used to determine the region of H2B which contained a putative nuclear localization sequence. Production of the expected β-galactosidase fusion proteins in yeast was verified by SDS-polyacrylamide gel electrophoresis and Western blot analysis, which demonstrated that the β-galactosidase fusion proteins had the expected molecular weights as predicted from DNA sequence (data not shown; Fig. 4).

Deletions from the carboxy terminus of H2B revealed a transition from nuclear to cytoplasmic localization of β-galactosidase fusion proteins between amino acids 28 and 33 of H2B (Fig. 2). This transition occurs in a basic region of the H2B amino terminus immediately preceding the H2A interaction domain (amino acids 40 to 117) (37, 51). To determine whether the region from amino acids 28 to 33 is uniquely required for H2B nuclear localization, fusion genes containing internal H2B sequences were constructed by using the

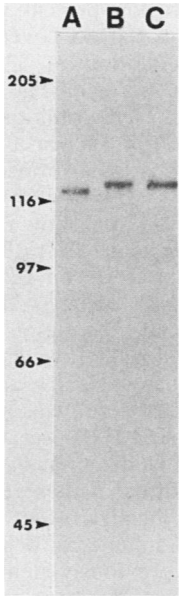

FIG. 4. Western blot analysis of H2B-β-galactosidase fusion protein immunoprecipitates. GRF-167 cells containing either pLGD5 (18), pFB1-33c, or pFB1-33K31→Mc were grown on minimal media minus uracil containing 2% galactose. Samples were immunoprecipitated (36), electrophoresed on 7.5% SDS-polyacrylamide gel electrophoresis, and subjected to Western blot analysis (3, 30, 50). Lanes: A, β-galactosidase; B, 33-amino-acid H2B-β-galactosidase; C, 33-amino-acid H2B-β-galactosidase containing a lysine-31-to-methionine substitution. Values at left are molecular weights (10^3).

iso-1-cytochrome *c* gene (*CYC1*) promoter and methionine start codon (18). Fusion proteins containing either amino acids 34 to 80 or 80 to 130 of H2B were cytoplasmic by indirect immunofluorescence (Fig. 2). These results indicate that either a sequence from amino acids 28 to 33 or a larger domain within the first 33 amino acids is responsible for H2B nuclear localization.

The region encompassing amino acids 28 to 33 was further characterized by constructing additional fusion proteins with amino-terminal H2B deletions (Fig. 4). A 33-amino-acid H2B-β-galactosidase fusion protein with a deletion of amino acids 2 to 22 was nuclear localized. Taken with the previous deletion analysis (Fig. 2), this result delimited a nuclear localization domain to the short sequence from amino acids 23 to 33 (Thr Ser Thr Ser Thr Asp Gly Lys Lys Arg Ser).

Because the nuclear location signal of SV40 large T antigen is composed of a similar basic sequence (25, 26, 49), we tested the importance of these amino acids in the region 23 to 33 by introducing a point mutation (A to T) which changed lysine 31 to a methionine by using site-directed mutagenesis. The resulting amino acid substitution preserves the predicted α-helical secondary structure of this region (8, 43) but results in the loss of one positive charge. When examined by indirect immunofluorescence, the fusion protein containing this single-amino-acid change was localized to the cytoplasm (Fig. 3e and f). This result further confirmed that amino acids 28 to 33 of H2B contain information for its nuclear localization.

To determine whether differential proteolytic degradation of the H2B-β-galactosidase fusion proteins might affect their nuclear localization (Fig. 4), fusion proteins were immunoprecipitated from cells and analyzed by SDS-polyacrylamide gel electrophoresis. Both the 33-amino-acid H2B-β-galactosidase fusion protein (Fig. 4, lane B) and the 33-amino-acid H2B-β-galactosidase fusion protein with the lysine-31-to-methionine substitution (lane C) were detected at a size consistent with the addition of 33 amino acids to β-galactosidase (lane A). No significant degradation of either fusion protein was observed. Additional quantitation of the intracellular distribution of nuclear and cytoplasmically localized fusion proteins was performed by immunoelectron microscopy (see below).

The data presented in Fig. 2 show that no other region of H2B other than amino acids 28 to 33 contains a nuclear localization signal. Therefore, an H2B-β-galactosidase fusion protein containing the entire H2B polypeptide but with a lysine-31-to-methionine substitution would be expected to be cytoplasmically localized. However, this H2B-β-galactosidase fusion protein was nuclear localized when expressed in yeast. This unexpected result was investigated further by examining 130-amino-acid H2B-β-galactosidase fusion proteins with amino-terminal deletions of residues 2 to 22, 14 to 31, and 1 to 33. All three of these β-galactosidase fusion proteins were nuclear localized (Fig. 5). The nuclear localization of the 1- to 33-amino-acid deletion was particularly unexpected, since the previously identified nuclear localization sequence is removed. However, in contrast to either the 34 to 80 or the 80 to 130 amino acid H2B-β-galactosidase fusion proteins which were cytoplasmically localized, this nuclear-localized fusion protein contains the entire H2A interaction region (amino acids 40 to 117) (37, 51). Therefore, analysis of H2B-β-galactosidase fusion proteins shows that H2B nuclear localization is dependent on either the amino-terminal sequence from amino acids 28 to 33 or an intact H2A interaction region.

Immunocytochemical localization of H2B-β-galactosidase fusion proteins. The subcellular localization of H2B-β-galactosidase fusion proteins was examined at greater resolution by electron microscopy. Thin sections were prepared from cells lacking β-galactosidase, or producing cytoplasmically localized or nuclear-localized H2B-β-galactosidase, as determined by indirect immunofluorescence. After etching the embedment to expose antigenic sites, the sections were treated with 10-nm colloidal gold-conjugated antibodies to visualize β-galactosidase and examined by transmission electron microscopy (Fig. 6A to D). The presence of 10-nm gold particles on the sections represented the localization of the β-galactosidase fusion proteins. There was no staining in cells which lack β-galactosidase (Fig. 6A). This lack of background staining permitted an accurate quantitation of the subcellular localization of β-galactosidase. Cells producing either β-galactosidase alone or a seven-amino-acid H2B-β-galactosidase fusion protein exhibited a majority of the gold particles in the cytoplasm (Fig. 6B), in agreement with the indirect immunofluorescence results (Fig. 2, 3, and 5). Similarly, cells containing a nuclear-localized 67-amino-acid H2B-β-galactosidase fusion exhibited predominantly nuclear staining (Fig. 6C).

The subcellular distribution of 10-nm gold particles was quantitated in a number of cell sections. The distribution of either β-galactosidase or a seven-amino-acid H2B-β-galactosidase fusion protein is essentially random, with 74 to 78% of the gold particles in the cytoplasm and 22 to 26% of the gold particles in the nucleus (the volume of the nucleus is approximately 25% of the total cell volume; Table 1). Thus, β-galactosidase is not nuclear excluded in yeast as defined by this technique. However, the subcellular distribution of gold particles is strikingly different in cells containing the 67-amino-acid H2B-β-galactosidase fusion protein, with the fusion protein predominating inside the nucleus (88%; Table 1).

The subcellular localization of the 33-amino-acid fusion protein and the 33-amino-acid fusion protein with a lysine-31-to-methionine substitution were also examined by electron microscopy. The 33-amino-acid fusion protein was predominantly nuclear localized (62% nuclear), whereas the 33-amino-acid lysine-31-methionine fusion protein was cytoplasmically localized (84% cytoplasmic; Table 1). Hence, a single-amino-acid substitution significantly changed the nuclear localization of this protein. In summary, electron microscopy generally verified the light microscopy data. The

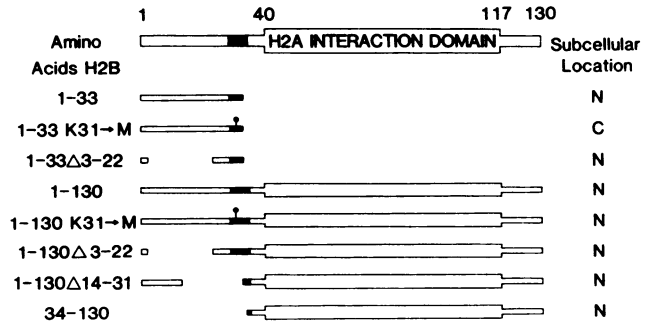

FIG. 5. Summary of the subcellular location of H2B-β-galactosidase fusion proteins containing amino-terminal deletions and a point mutation. Schematic drawing of H2B shows nuclear localization sequence (black box) and H2A interaction domain (33, 37, 51). The location of the lysine-31-to-methionine substitution is shown by ♦ Subcellular location determined by indirect immunofluorescence was either nuclear (N) or cytoplasmic (C). Constructions are described in Materials and Methods (Fig. 1).

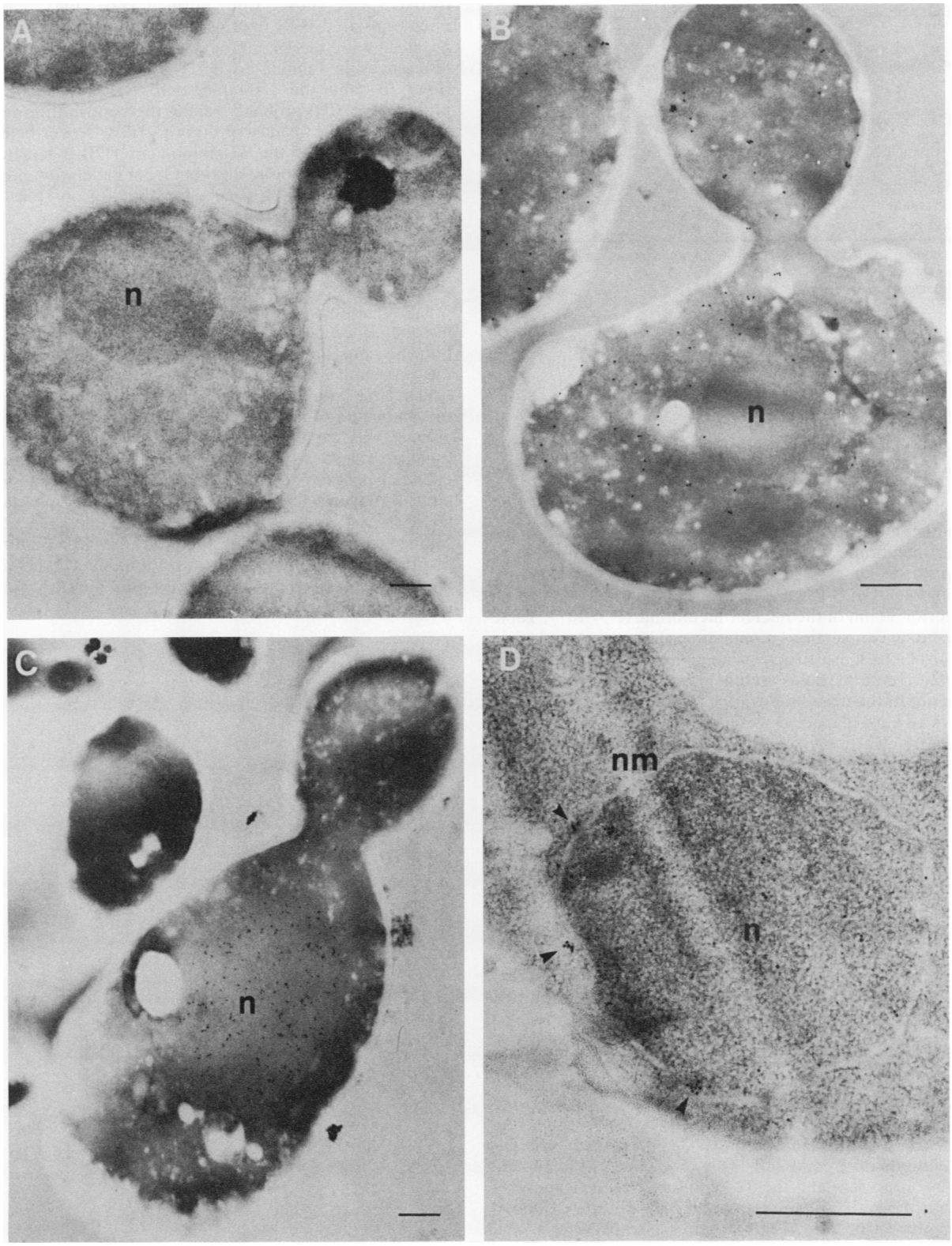

FIG. 6. Localization of H2B-β-galactosidase fusion proteins by electron microscopy. GRF-167 cells containing no plasmid, pFB1-7c, or pFB1-67c were grown on minimal media minus uracil containing 2% galactose. Panels: A, no β-galactosidase; B, 7-amino-acid H2B-β-galactosidase fusion protein; C, 67-amino-acid H2B-β-galactosidase fusion protein; D, enhanced view of nucleus in a cell producing a 67-amino-acid H2B-β-galactosidase fusion protein. Arrows denote the clusters of gold particles at the nuclear-cytoplasmic interface. Bar, 0.5 μm.

TABLE 1. Quantitation of 10-nm gold particle distribution in yeast cell thin sections

Fusion protein	No. of cell sections	No. of gold particles in:			
		Nucleus	Cytoplasm	Nuclear membrane[a]	
				Interior	Exterior
β-Gal[b]	21	936	3,054	259	294
1–7 H2B-β-gal	40	310	1,264	75	75
1–67 H2B-β-gal	26	1,945	251	331	55
1–33 H2B-β-gal	25	714	458	113	49
1–33 K31 →M H2B-β-gal	25	116	706	16	34

[a] The number of gold particles within 30 nm of the interior or exterior of the nuclear membrane.
[b] Gal, Galactosidase.

immunocytochemical staining in conjunction with electron microscopy demonstrated that, at high resolution, the exact subcellular location of the fusion proteins was not exclusively cytoplasmic or nuclear.

In approximately 10% of the sections containing nuclear-localized fusion proteins, closer inspection of nuclei revealed clusters of five to eight gold particles near the nuclear-cytoplasmic interface (Fig. 6D). These clusters could be observed on either side of the nuclear membrane. When the number of gold particles within 30 nm of the nuclear membrane was quantitated, a significant number of gold particles in sections containing the nuclear-localized 67-amino-acid H2B-β-galactosidase fusion protein were on the interior 30 nm of the nuclear membrane ($P < 10^{-8}$; Table 1). In contrast, sections containing the two cytoplasmic H2B-β-galactosidase fusion proteins showed a random distribution of gold particles within 30 nm of either the interior or exterior of the nuclear envelope ($P = 0.55$; Table 1). Since clusters of gold particles were observed only in cells expressing nuclear-localized β-galactosidase fusion proteins, they may represent intermediate steps in the nuclear localization process (12).

DNA-binding properties of H2B-β-galactosidase fusion proteins. To investigate possible differences in nonspecific DNA binding between nuclear-excluded and nuclear-localized fusion proteins, the in vitro binding of several such fusion proteins to dsDNA cellulose was examined. mRNA was transcribed from plasmid templates (pSPZA33, pSPZA33K31→M, and pSPZA130) for both the 33-amino-acid fusion protein as well as the 33-amino-acid point mutation fusion protein, a full-length (130-amino-acid) H2B-β-galactosidase fusion protein, and a β-galactosidase control (pSPZRR) by using SP6 RNA polymerase. The proteins translated in vitro by using a rabbit reticulocyte lysate had molecular weights as determined by SDS-polyacrylamide gel electrophoresis consistent with their expected molecular weights (data not shown). The translated proteins were bound to dsDNA cellulose and eluted with stepwise increasing salt concentrations. As shown, the β-galactosidase control fusion protein was entirely eluted with 20 mM NaCl (Fig. 7A). The 33-amino-acid H2B fusion protein and the 33-amino-acid H2B fusion protein with the lysine-31-to-methionine substitution exhibited similar elution profiles (Fig. 7B and C, respectively), and both H2B fusion proteins exhibited some eluted protein at 100 mM NaCl in contrast to the β-galactosidase control fusion protein. The 130-amino-acid H2B-β-galactosidase fusion protein eluted at higher salt concentrations (200 mM; Fig. 7D) than the other H2B-β-galactosidase fusion proteins. The lower-molecular-weight bands in this sample are probably prematurely terminating protein products as they bind to dsDNA cellulose. Both purified H2B (Fig. 7E) and in vitro-translated H2B (data not shown) had identical elution profiles, with the major peak eluting at 1 M NaCl. The differences in binding to dsDNA cellulose between H2B (Fig. 7E) and the 130-amino-acid β-galactosidase fusion protein (Fig. 7D) probably reflect the contribution of fusing the large β-galactosidase protein to H2B. Nevertheless, the elution profiles of the 33-amino-acid H2B-β-galactosidase fusion proteins are quite different from the elution profiles of a 130-amino-acid H2B-β-galactosidase fusion (Fig. 7D) or the full-length H2B protein (Fig. 7E).

DISCUSSION

These studies demonstrate that two regions of yeast histone 2B are important in determining its nuclear localization. By constructing *H2B-lacZ* gene fusions and examining the subcellular localization of the H2B-β-galactosidase fusion proteins produced in yeast, either a specific sequence in the amino terminus of H2B or an intact H2A interaction domain was capable of localizing the cytoplasmic protein β-galactosidase to the nucleus. The amino-terminal sequence has homology to the nuclear location signal in SV40 large T antigen (H2B-Gly29-Lys Lys Arg Ser Lys Ala; SV40 large T-Pro-126 Lys Lys Lys Arg Lys Val) (25, 26, 49). Mutagenesis of H2B lysine 31 to an uncharged amino acid residue abolished nuclear localization, thus indicating the importance in nuclear targeting of this amino acid in the short sequence.

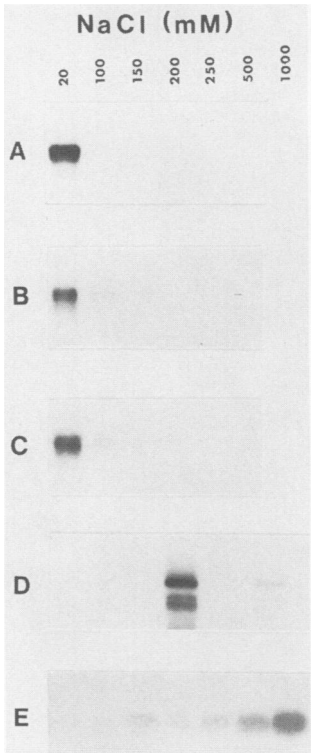

FIG. 7. Binding of β-galactosidase fusion proteins to dsDNA cellulose. Panels: A, rpL3 5-amino-acid β-galactosidase fusion protein; B, 33-amino-acid H2B-β-galactosidase fusion protein; C, 33-amino-acid H2B-β-galactosidase fusion protein containing lysine-31-to-methionine substitution; D, 130-amino-acid H2B-β-galactosidase fusion protein; E, purified yeast H2B.

TABLE 2. List of predicted H2B nuclear localization sequences

H2B[a]	Predicted nuclear localization sequence[b]	Predicted secondary structure[c]
H2B1 *S. cerevisiae*	28 DGKKRKSKAK	α-Helix
Fruit fly	23 TDKKKKRKRK	α-Helix
Sea urchin sperm (*Parenchinus angulosus*)	22 GGKKRHRKRK	α-Helix
Sea urchin H2B1 (embryonic; *Psammechinus miliaris*)	22 GGKKRNRKRK	β-Turn
Starfish sperm	20 SDKKRRRKRK	α-Helix
Limpet gonad	21 GDKKRKRRRK	α-Helix
Toad (*Xenopus laevis*)	21 TQKKGDKKRM	β-Turn and α-helix
Crocodile	25 GDKKRMNSFK	α-Helix
Rainbow trout	23 GGKKRKRSRK	β-Turn and α-helix
Chicken	25 GDKKRKKSRK	β-Turn and α-helix
Mouse, cow, and human	25 DGKKRKRSRK	None

[a] Sequences obtained from the U.S. National Biomedical Research Foundation data base include H2Bs from fungi, insects, mollusks, echinoderms, reptiles, birds, fish, and mammals.

[b] The number preceding the sequence indicates the position of the first amino acid. Single letter amino acid codes: A, Ala; D, Asp; G, Gly, H, His; K, Lys; M, Met; N, Asn; Q, Gln; R, Arg; S, Ser; and T, Thr.

[c] Secondary structure predictions were made by the methods of Chou and Fasman (10, 43).

The discovery of two nuclear location signals in polyomavirus large T antigen (44) prompted us to determine whether the region from amino acids 28 to 33 was the only nuclear localization sequence in H2B. H2B-β-galactosidase fusion proteins containing the internal amino acids 34 to 80 or 80 to 130 of H2B were cytoplasmic by indirect immunofluorescence when expressed in yeast. Whereas there might be a nuclear localization domain that overlaps these two separated regions, these results suggest that there is no other short amino acid sequence in H2B that can act as a nuclear localization sequence.

Amino acids 3 to 32 or 30 to 37 can be deleted from yeast H2B without impairment of cell growth (46, 52). Consequently, amino acids 28 to 33, which were identified as important for nuclear localization of H2B, are dispensable in vivo. This paradox was examined by constructing 130-amino-acid H2B-β-galactosidase fusions that contained either amino-terminal deletions or a lysine-31-to-methionine change. All of these fusion proteins were nuclear localized by indirect immunofluorescence. The H2A interaction region of calf thymus H2B is contained within residues 37 to 114 as determined by nuclear mass resonance spectroscopy (37). A homologous region is contained within residues 40 to 119 of yeast H2B (51). Although it may be possible that a nuclear localization signal-defective H2B diffuses into the nucleus and is retained by interaction with H2A, we favor a model in which H2A and H2B are cotransported into the nucleus as a heterodimer. Thus, if either H2A or H2B in an oligomeric complex contained a signal, the complex would be nuclear targeted. The rate of nuclear transport is related to the number of signals in an oligomeric complex (11), and the presence of two signals in an H2A-H2B dimer may facilitate the rapid histone influx required during the interval of DNA replication.

Histones are small basic proteins (15 kilodaltons), and their nuclear localization may result from diffusion into the nucleus, and subsequent nonspecific binding to DNA (4, 6). If the primary function of the nuclear localization sequence was DNA binding, then the content of basic amino acids contributed by H2B to the fusion protein would be expected to correlate with nuclear localization. A nuclear-localized 33-amino-acid H2B fusion protein differs from a cytoplasmically localized 33-amino-acid H2B fusion protein with a lysine-31-to-methionine substitution by one positive charge. Although this difference does not seem great enough to cause relocation of the protein if nonspecific DNA binding alone were important, we tested this possibility by examining the binding to dsDNA cellulose of fusion proteins translated in vitro. Both the 33-amino-acid H2B-β-galactosidase fusion protein and the 33-amino-acid H2B fusion protein containing a lysine-31-to-methionine substitution eluted similarly from dsDNA cellulose, indicating that, by this in vitro assay, single charge changes did not significantly affect DNA binding (Fig. 7). In addition, the nuclear localization of H2B-β-galactosidase fusion proteins was dependent on specific sequences rather than the number of basic amino acids contributed by H2B. For example, the 33-amino-acid fusion protein with a lysine-31-to-methionine substitution (10 basic amino acids) is not nuclear localized, whereas the 33-amino-acid H2B fusion protein with a deletion of amino acids 2 to 22 (3 basic amino acids) is nuclear localized. Thus, the nuclear localization of H2B fusion proteins is correlated with the specific amino acid sequence from amino acids 28 to 33 of H2B and not the number of basic amino acids, as would be expected if nonspecific DNA binding determined the nuclear localization of these fusion proteins. Similarly, it has been

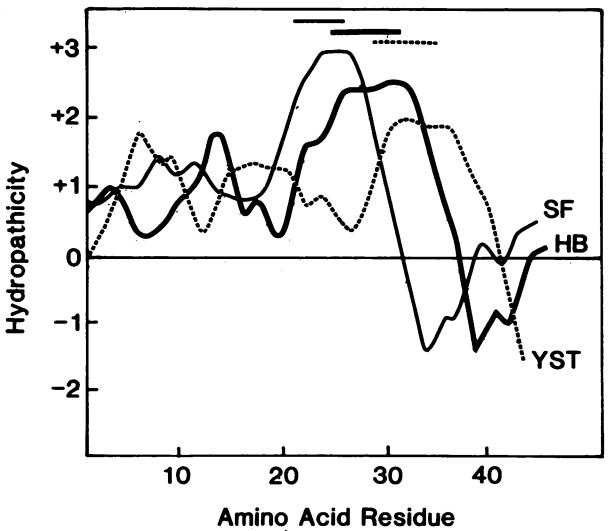

FIG. 8. Hydropathicity plot of amino acids 1 to 45 in H2B from several species: HB, human-beef H2B; SF, starfish sperm H2B; YST, yeast H2B-1. Positions of predicted nuclear localization sequences are shown above the hydropathicity curves. Note the transition from hydrophilic to hydrophobic domains immediately after the nuclear localization sequences.

shown that DNA binding was not sufficient for nuclear localization of either SV40 large T antigen (41) or the yeast GAL4 protein (48). Kinetic experiments have aided in resolving the issue of nonspecific diffusion and nuclear retention and specific transport (9, 11, 12, 15, 29). The inability to determine accurate kinetic measurements in yeast makes it difficult to distinguish between passive diffusion with subsequent nuclear retention and active uptake into the nucleus by these methods.

Studies of nuclear localization have used *E. coli* β-galactosidase as a nonnuclear test protein because its large molecular size (116-kilodalton monomer) should preclude its nonspecific diffusion into the nucleus (19, 26, 36, 47). Consistent with these studies, we find that by indirect immunofluorescence β-galactosidase has a cytoplasmic localization when expressed in yeast. However, when thin sections of yeast cells expressing β-galactosidase or a seven-amino-acid H2B-β-galactosidase fusion protein were examined by immunocytochemical staining using electron microscopy, 22 to 26% of the immunoreactive material was found in the nucleus. Thus, β-galactosidase is not entirely nuclear excluded in yeast. The lack of nuclear exclusion of β-galactosidase fusion proteins in Vero cells has been attributed to proteolysis (26). Although proteolysis of β-galactosidase may contribute to its nuclear localization in yeast, the amount of degradation of β-galactosidase fusion proteins as determined by Western blot analysis (Fig. 4; data not shown) cannot account for all (26%) of the β-galactosidase in the nucleus. Nonetheless, those fusion proteins which are nuclear localized by indirect immunofluorescence are predominantly inside the nucleus when examined by electron microscopy.

In an attempt to identify similar nuclear localization sequences in H2Bs from other species, 11 different H2Bs were examined by both primary sequence homology and Chou and Fasmann secondary structure analysis (10, 43). A list of these sequences is shown in Table 2. Both yeast H2B (amino acids 30 to 38) and SV40 large T antigen (amino acids 127 to 134) (28) have a predicted α-helical structure in the region that comprises their nuclear localization sequence. Candidate nuclear localization sequences in 8 of 11 H2Bs fall in a region with the predicted α-helical structure. However, in three H2B species, including human H2B, potential localization sequences did not contain a predicted α-helical structure. As an additional measure of secondary structure, we performed a hydropathicity analysis (27, 43). The hydropathicity plot of yeast H2B showed that the nuclear localization sequence occurred at a characteristic point in the hydrophilic to hydrophobic transition in the first 45 amino acids (Fig. 8). Similar hydropathicity plots were used to predict where nuclear localization sequences for sea urchin and human H2B might be found. Thus, using these combined analyses, nuclear localization sequences for H2Bs from a wide range of organisms can be predicted (Table 2).

We have shown that yeast H2B combines features which have been previously identified as important in nuclear protein targeting: (i) a specific localization sequence, and (ii) the dispensability of such a sequence if the protein forms a complex with another protein with a nuclear localization signal. Further elucidation of the mechanism of nuclear transport will be necessary to understand how these features function together.

ACKNOWLEDGMENTS

We thank Jennifer McKnight for the generous gift of rabbit anti-β-galactosidase antibody, Fran Parks at Genex for performing the oligonucleotide-directed mutagenesis, Michael Caine for excellent technical assistance, Howard Fried, Leonard Guarente, Michael Gruenstein, Roy Parker, Tillman Schuster, and John Teem for gifts of plasmids, Gerry Fink and David Norris for gifts of yeast strains, and Mary Ann Osley for a critical reading of the manuscript.

This work was supported in part by Public Health Service grants GM33332, RR05526 (L.M.H.), CA37667 and SO7 RR05526-24 (R.L.G.), and HD18066 (R.H.S.) from the National Institutes of Health, American Cancer Society grant ACS-118C (L.M.H.), and Damon Runyon-Walter Winchell Cancer Fund Fellowship DRW628 (R.B.M.).

ADDENDUM IN PROOF

A recent report regarding intracellular localization of histone mRNA has been called to our attention (J. B. Lawrence, R. H. Singer, C. A. Villnave, J. L. Stein, and G. S. Stein, Proc. Nat'l. Acad. Sci. USA, in press). It was found that H1 and H4 mRNAs were distributed throughout the cell cytoplasm and not localized around the nucleus. Hence, determinants within the histone proteins themselves must be responsible for their nuclear localization.

LITERATURE CITED

1. **Adams, A. E. M., and J. R. Pringle.** 1983. Relationship of actin and tubulin distribution to bud growth in wild-type and morphogenetic mutant *Saccharomyces cerevisiae*. J. Cell Biol. **98**:938–945.
2. **Bendayan, M., and M. Zollinger.** 1983. Ultrastructural localization of antigenic sites on osmium-fixed tissues applying the protein A-gold technique. J. Histochem. Cytochem. **31**:101–109.
3. **Blake, M. S., K. H. Johnston, G. H. Russell-Jones, and E. C. Gotschlich.** 1984. A rapid and sensitive method for detection of alkaline phosphatase conjugated antibody on Western blots. Anal. Biochem. **136**:175–179.
4. **Bonner, W. M.** 1975. Protein migration into nuclei. I. Frog oocyte nuclei accumulate microinjected histones, allow entry to small proteins, and exclude large proteins. J. Cell Biol. **64**:421–430.
5. **Bonner, W. M.** 1975. Protein migration into nuclei. II. Frog oocyte nuclei accumulate a class of microinjected oocyte nuclear proteins and exclude a class of microinjected oocyte cytoplasmic proteins. J. Cell Biol. **64**:431–437.
6. **Bonner, W. M.** 1978. Protein migration and accumulation in nuclei, p. 97–148. *In* H. Busch (ed.), The cell nucleus, vol. 6, part C. Academic Press, Inc., New York.
7. **Botstein, D., S. C. Falco, S. S. Stewart, M. Brennan, S. Scherer, D. T. Stinchcomb, K. Struhl, and R. Davis.** 1979. Sterile host yeasts: a eukaryotic system of biological contaminant for recombinant DNA experiments. Gene **8**:17–24.
8. **Chou, P. Y., and G. D. Fasman.** 1978. Empirical prediction of protein conformation. Annu. Rev. Biochem. **47**:251–276.
9. **Davey, J., N. J. Dimmock, and A. Colman.** 1985. Identification of the sequence responsible for nuclear accumulation of the influenza virus nucleoprotein in *Xenopus* oocytes. Cell **40**:667–675.
10. **De Robertis, E. M., R. F. Longthorne, and J. B. Gurdon.** 1978. Intracellular migration of nuclear proteins in *Xenopus* oocytes. Nature (London) **272**:254–256.
11. **Dingwall, C., S. V. Sharnick, and R. A. Laskey.** 1982. A polypeptide domain that specifies migration of nucleoplasmin to the nucleus. Cell **30**:449–458.
12. **Feldherr, C. M., E. Kallenbach, and N. Schultz.** 1984. Movement of a karyophilic protein through the nuclear pores of oocytes. J. Cell Biol. **99**:2216–2222.
13. **Fried, H. M., H. G. Nam, S. Loechel, and J. Teem.** 1985. Characterization of yeast strains with conditionally expressed variants of ribosomal protein genes *tcm1* and *cyh2*. Mol. Cell. Biol. **5**:99–108.
14. **Gillam, S., C. R. Astell, and M. Smith.** 1980. Site specific mutagenesis using oligodeoxyribonucleotides: isolation of a phenotypically silent ϕX174 mutant, with a specific nucleotide deletion, at high frequency. Gene **12**:129–137.
15. **Goldfarb, D. S., J. Gariepy, G. Schoolnik, and R. D. Kornberg.**

1986. Synthetic peptides as nuclear localization signals. Nature (London) **322**:641–644.
16. **Gosselin, E.** 1984. Unlabeled antibody methods in electron microscopy: a comparison of single and multistep procedures using colloidal gold. J. Histochem. Cytochem. **32**:799–804.
17. **Guarente, L., G. Lauer, T. M. Roberts, and M. Ptashne.** 1980. Improved methods for maximizing expression of a cloned gene: a bacterium that synthesizes rabbit β-globin. Cell **20**:543–553.
18. **Guarente, L., R. Yocum, and P. Gifford.** 1982. A *GAL10-CYC1* hybrid yeast promoter identifies the GAL4 regulatory region as an upstream site. Proc. Natl. Acad. Sci. USA **79**:7410–7414.
19. **Hall, M. N., L. M. Hereford, and I. Herskowitz.** 1984. Targeting of *E. coli* β-galactosidase to the nucleus in yeast. Cell **36**:1057–1065.
20. **Hereford, L., S. Bromley, and M. A. Osley.** 1982. Periodic transcription of yeast histone genes. Cell **30**:305–310.
21. **Hereford, L. M., K. Fahrner, J. Woolford, Jr., M. Rosbash, and D. B. Kaback.** 1979. Isolation of yeast histone genes H2A and H2B. Cell **18**:1261–1271.
22. **Hereford, L. M., M. A. Osley, J. R. Ludwig II, and C. S. McLaughlin.** 1981. Cell-cycle regulation of yeast histone mRNA. Cell **24**:367–375.
23. **Isenberg, I.** 1979. Histones. Annu. Rev. Biochem. **48**:159–191.
24. **Ito, H., Y. Fukuda, K. Murata, and A. Kimura.** 1983. Transformation of intact yeast cells treated with alkali cations. J. Bacteriol. **153**:163–168.
25. **Kalderon, D., W. D. Richardson, A. F. Markham, and A. E. Smith.** 1984. Sequence requirements for nuclear localisation of SV40 large T antigen. Nature (London) **311**:33–38.
26. **Kalderon, D., B. L. Roberts, W. D. Richardson, and A. E. Smith.** 1984. A short amino acid sequence able to specify nuclear location. Cell **39**:499–509.
27. **Kyte, J., and R. F. Doolittle.** 1982. A simple method for displaying the hydropathic character of a protein. J. Mol. Biol. **157**:105–132.
28. **Lanford, R. E., and J. S. Butel.** 1984. Construction and characterization of an SV40 mutant defective in nuclear transport of T antigen. Cell **37**:801–813.
29. **Lanford, R. E., P. Kanda, and R. C. Kennedy.** 1986. Induction of nuclear transport with a synthetic peptide homologous to the SV40 T antigen transport signal. Cell **46**:575–582.
30. **Leary, J. J., D. J. Brigati, and D. C. Ward.** 1983. Rapid and sensitive colorimetric method for visualizing biotin-labeled DNA probes hybridized to DNA or RNA immobilized on nitrocellulose: bioblots. Proc. Natl. Acad. Sci. USA **80**: 4045–4049.
31. **Maniatis, T., E. F. Fritsch, and J. Sambrook.** 1982. Molecular cloning: a laboratory manual. Cold Spring Harbor Laboratory, Cold Spring Harbor, New York.
32. **Mardian, J. K. W., and I. Isenberg.** 1978. Yeast inner histones and evolutionary conservation of histone-histone interactions. Biochemistry **17**:3825–3833.
33. **McGhee, J. D., and G. Felsenfeld.** 1980. Nucleosome structure. Annu. Rev. Biochem. **49**:1115–1156.
34. **Melton, D. A., P. A. Krieg, M. R. Rebagliati, T. Maniatis, K. Zinn, and M. R. Green.** 1984. Efficient in vitro synthesis of biologically active RNA and DNA hybridization probes from plasmids containing the bacteriophage SP6 promoter. Nucleic Acids Res. **18**:7035–7056.
35. **Messing, J., R. Crea, and P. H. Seeburg.** 1981. A system for shotgun DNA sequencing. Nucleic Acids Res. **9**:309–321.
36. **Moreland, R. B., H. G. Nam, L. M. Hereford, and H. M. Fried.** 1985. Identification of a nuclear localization signal of a yeast ribosomal protein. Proc. Natl. Acad. Sci. USA **82**:6561–6565.
37. **Moss, T., P. D. Cary, B. D. Abercrombie, C. Crane-Robinson, and E. M. Bradbury.** 1976. A pH-dependent interaction between histones H2A and H2B involving secondary and tertiary folding. Eur. J. Biochem. **71**:337–350.
38. **Osley, M A., J. Gould, S. Y. Kim, M. Kane, and L. Hereford.** 1986. Identification of sequences in a yeast histone promoter involved in periodic transcription. Cell **45**:537–544.
39. **Osley, M. A., and L. M. Hereford.** 1982. Identification of a sequence responsible for periodic synthesis of yeast histone 2A mRNA. Proc. Natl. Acad. Sci. USA **79**:7689–7693.
40. **Paine, P. L., L. C. Moore, and S. B. Horowitz.** 1975. Nuclear envelope permeability. Nature (London) **254**:109–114.
41. **Paucha, E., D. Kalderon, W. D. Richardson, R. W. Harvey, and A. E. Smith.** 1985. The abnormal location of cytoplasmic SV40 large T is not caused by failure to bind to DNA or to p53. EMBO J. **4**:3235–3240.
42. **Peters, R.** 1984. Nucleocytoplasmic flux and intracellular mobility in single hepatocytes measured by fluorescence microphotolysis. EMBO J. **3**:1831–1836.
43. **Pustel, J., and F. C. Kafatos.** 1984. A convenient and adaptable package of computer programs for DNA and protein sequences management. Nucleic Acids Res. **12**:643–655.
44. **Richardson, W. D., B. L. Roberts, and A. E. Smith.** 1986. Nuclear location signals in polyoma virus large-T. Cell **44**: 77–85.
45. **Sanger, F., S. Nicklen, and A. R. Coulson.** 1977. DNA sequencing with chain-terminating inhibitors. Proc. Natl. Acad. Sci. USA **74**:5463–5467.
46. **Schuster, T., M. Han, and M. Grunstein.** 1986. Yeast histone H2A and H2B amino termini have interchangeable functions. Cell **45**:445–451.
47. **Silver, P. A., R. Brent, and M. Ptashne.** 1986. DNA binding is not sufficient for nuclear localization of regulatory proteins in *Saccharomyces cerevisiae*. Mol. Cell. Biol. **6**:4763–4766.
48. **Silver, P. A., L. P. Keegan, and M. Ptashne.** 1984. Amino terminus of yeast GAL4 gene product is sufficient for nuclear localization. Proc. Natl. Acad. Sci. USA **81**:5951–5955.
49. **Smith, A. E., D. Kalderon, B. L. Roberts, W. D. Colledge, M. Edge, P. Gillet, A. F. Markham, E. Paucha, and W. D. Richardson.** 1985. The nuclear location signal. Proc. R. Soc. Lond. B **226**:43–58.
50. **Towbin, H., T. Staehelin, and J. Gordon.** 1979. Electrophoretic transfer of proteins from polyacrylamide gels to nitrocellulose sheets. Procedures and some applications. Proc. Natl. Acad. Sci. USA **76**:4350–4354.
51. **Wallis, J. W., L. M. Hereford, and M. Gruenstein.** 1980. Histone H2B genes of yeast encode two different proteins. Cell **22**:799–805.
52. **Wallis, J. W., M. Ryowski, and M. Gruenstein.** 1983. Yeast histone H2B containing large amino terminus deletions can function *in vivo*. Cell **35**:711–719.